Sequestration of microRNA-mediated target repression by the Ago2-associated RNA-binding protein FAM120A

TIMOTHY J. KELLY,[1,4,5] HIROSHI I. SUZUKI,[1,4] JESSE R. ZAMUDIO,[1,2] MEGUMU SUZUKI,[1] and PHILLIP A. SHARP[1,3]

[1]David H. Koch Institute for Integrative Cancer Research, Massachusetts Institute of Technology, Cambridge, Massachusetts 02139, USA
[2]Department of Molecular, Cell, and Developmental Biology, University of California, Los Angeles, Los Angeles, California 90095, USA
[3]Department of Biology, Massachusetts Institute of Technology, Cambridge, Massachusetts 02139, USA

ABSTRACT

Argonaute (Ago) proteins interact with various binding partners and play a pivotal role in microRNA (miRNA)-mediated silencing pathways. By utilizing immunoprecipitation followed by mass spectrometry to determine cytoplasmic Ago2 protein complexes in mouse embryonic stem cells (mESCs), we identified a putative RNA-binding protein FAM120A (also known as OSSA/C9ORF10) as an Ago2 interacting protein. Individual nucleotide resolution cross-linking and immunoprecipitation (iCLIP) analysis revealed that FAM120A binds to homopolymeric tracts in 3′-UTRs of about 2000 mRNAs, particularly poly(G) sequences. Comparison of FAM120A iCLIP and Ago2 iCLIP reveals that greater than one-third of mRNAs bound by Ago2 in mESCs are co-bound by FAM120A. Furthermore, such FAM120A-bound Ago2 target genes are not subject to Ago2-mediated target degradation. Reporter assays suggest that the 3′-UTRs of several FAM120A-bound miRNA target genes are less sensitive to Ago2-mediated target repression than those of FAM120A-unbound miRNA targets and FAM120A modulates them via its G-rich target sites. These findings suggest that Ago2 may exist in multiple protein complexes with varying degrees of functionality.

Keywords: microRNA; Ago2; FAM120A; iCLIP

INTRODUCTION

MicroRNAs (miRNAs) are versatile regulators of gene expression and are generated by a multistep biogenesis pathway (Suzuki and Miyazono 2011; Treiber et al. 2019). In the canonical pathway for miRNA biogenesis, long primary miRNA transcripts (pri-miRNAs) are processed to hairpin-structured precursor miRNAs (pre-miRNAs) by the nuclear Drosha and DGCR8 complex. Pre-miRNAs are further processed into 21- to 24-nt double-stranded miRNAs through the activity of Dicer. Resultant miRNA duplexes are loaded into Argonaute (Ago) proteins (Ago1–Ago4 in mammals), and one strand is retained in Ago and serves as the mature miRNA strand (Suzuki et al. 2015). Then, the RNA-induced silencing complex (RISC), of which the minimal components are Ago and miRNA, directs miRNA-mediated target repression.

Ago proteins are known to interact with a variety of protein-binding partners and play central roles in miRNA-mediated silencing pathways. These functions are mediated by at least two functionally distinct complexes. In the RISC-loading complex (RLC), comprised of Ago2, Dicer, and TRBP, Ago is loaded with miRNA. This process is stimulated by auxiliary factors such as HSC70/HSP90 chaperone proteins. On the other hand, the miRNA-induced silencing complex (miRISC) includes TNRC6 proteins (TNRC6A/B/C), also known as GW182 proteins, and mediates posttranscriptional repression of target mRNAs (Braun et al. 2011; Chekulaeva et al. 2011; Fabian et al. 2011). TNRC6 proteins are core components of miRISC and induce shortening of the poly(A) tails of mRNAs by an association with the CCR4-NOT complex, subsequent translational repression, and mRNA destabilization. Several previous studies have identified multiple other Ago protein-binding partners in various cell types (Höck et al. 2007; Landthaler et al. 2008; Frohn et al. 2012; Li et al. 2014; Schopp et al. 2017).

[4]These authors contributed equally to this work.
[5]**Present address:** Cardiovascular and Metabolic Disease, Novartis Institutes for Biomedical Research (NIBR), Cambridge, Massachusetts 02139, USA
Corresponding author: sharppa@mit.edu
Article is online at http://www.rnajournal.org/cgi/doi/10.1261/rna.071621.119.

To accurately interrogate cytoplasmic Ago2 interacting proteins in mouse embryonic stem cells (mESCs), we performed immunoprecipitation followed by mass spectrometry in mESCs expressing a single epitope-tagged Ago family member in an Ago family knockout background (Zamudio et al. 2014). This study characterizes a putative RNA-binding protein FAM120A (also known as OSSA/C9ORF10) as a novel Ago2 interacting protein.

RESULTS

Identification of FAM120A as an Ago2 interacting protein

We have previously described an adapted mESC system that allows for doxycycline (Dox)-inducible expression of a single Ago protein in an Ago-deficient background to accurately analyze its function (Zamudio et al. 2014). TT-FHAgo1 or TT-FHAgo2 mESCs lack mouse Ago1–Ago4 (*Ago1−/−; Ago2−/−; Ago3−/−; Ago4−/−*) and express Flag-hemagglutinin (HA)-tagged human Ago1 (FHAgo1) or Ago2 (FHAgo2) under the control of a TRE-Tight (TT) Dox inducible promoter. After fractionation in TT-FHAgo1 and TT-FHAgo2 cells, FHAgo proteins were immunoprecipitated with anti-Flag and anti-HA antibodies and resultant protein complexes were analyzed by mass spectrometry (Supplemental Fig. S1A,B). As a control, we performed the same experiments using mESCs expressing untagged human Ago2 (TT-Ago2). Mass spectrometry analysis revealed various Ago1 or Ago2 interacting proteins as summarized in Figure 1A and Supplemental Table S1. These included many known Ago2 interacting partners such as HSP90, TNRC6B, UPF1, and IGF2BP2.

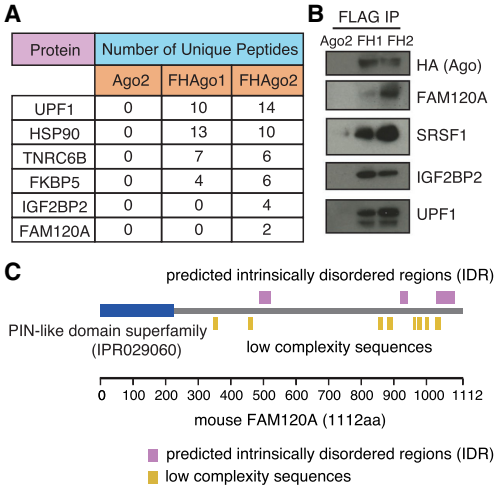

FIGURE 1. Ago2 interacts with FAM120A in the cytoplasm of mESCs. (*A*) Select list of proteins identified in Flag IP from cytoplasmic extracts from mESCs expressing Ago2, FHAgo1, or FHAgo2. (*B*) Ago2 binds to FAM120A in mESCs. (FH1) FHAgo1, (FH2) FHAgo2. (*C*) Schematic representation of FAM120A protein domains from Ensembl database.

We confirmed the interaction with SRSF1, IGF2BP2, UPF1, and FAM120A in an independent immunoprecipitation assay (Fig. 1B). Interestingly, FHAgo1 IP mass spectrometry analysis failed to identify FAM120A as an Ago1 interacting protein, and interaction between Ago1 and FAM120A was also very weak in the follow-up validation by immunoprecipitation (Fig. 1A,B). FAM120A has been reported to be an Ago2 interacting protein in two previous Ago2 interactome studies (Frohn et al. 2012; Schopp et al. 2017), however, whether or not this interaction has any functional consequence has not been characterized. Thus, we focused on FAM120A in the subsequent study. We observed that FAM120A is primarily distributed in the cytoplasm (Supplemental Fig. S1C) and that, similar to the RNA dependent interactions with UPF1 and IGF2BP2 (Supplemental Fig. S1D), Ago2–FAM120A interaction is RNA dependent (Supplemental Fig. S1E), suggesting enriched co-occupancy on cellular RNA targets. Figure 1C depicts FAM120A domain structure including a PIN-like domain at the amino terminus and several predicted intrinsically disordered regions and low complexity sequences in the middle and clustered near the carboxyl terminus.

RNA-binding properties of FAM120A

FAM120A is a poorly characterized protein that has been suggested to function as a regulator of activation of several intracellular kinases, including Src, FAK, and PI3K, following oxidative stress and IL13 receptor α2 signaling and has been shown to bind to RNA (Kobayashi et al. 2008; Tanaka et al. 2009; Kwon et al. 2013; Bartolome et al. 2015). To analyze FAM120A function, we generated mESCs expressing Flag-HA-tagged and untagged FAM120A (TT-FHFAM120A and TT-FAM120A) in a Dox-inducible manner (Supplemental Fig. S2A). In order to characterize the RNA species bound to FAM120A in mESCs, we utilized individual nucleotide resolution cross-linking and immunoprecipitation (iCLIP). TT-FAM120A and TT-FHFAM120A expressing cells were UV cross-linked, and FHFAM120A was enriched by utilizing tandem Flag and HA immunoprecipitation, followed by RNase I digestion, 5′ end labeling, and separation via SDS-PAGE. We observed that FHFAM120A clearly binds to RNAs that are not observed in the control IP from untagged FAM120A expressing cells (Supplemental Fig. S2B). iCLIP analysis yielded identification of about 11,000 clusters bound by FHFAM120A, which are statistically enriched against the untagged FAM120A iCLIP library. Further annotation revealed that, of the enriched RNA bound to FAM120A, >70% of the iCLIP clusters map to 3′-UTRs, corresponding to about 2000 bound genes (Fig. 2A–C). Gene ontology (GO) analysis of bound genes showed enrichment of various biological functions, including RNA-

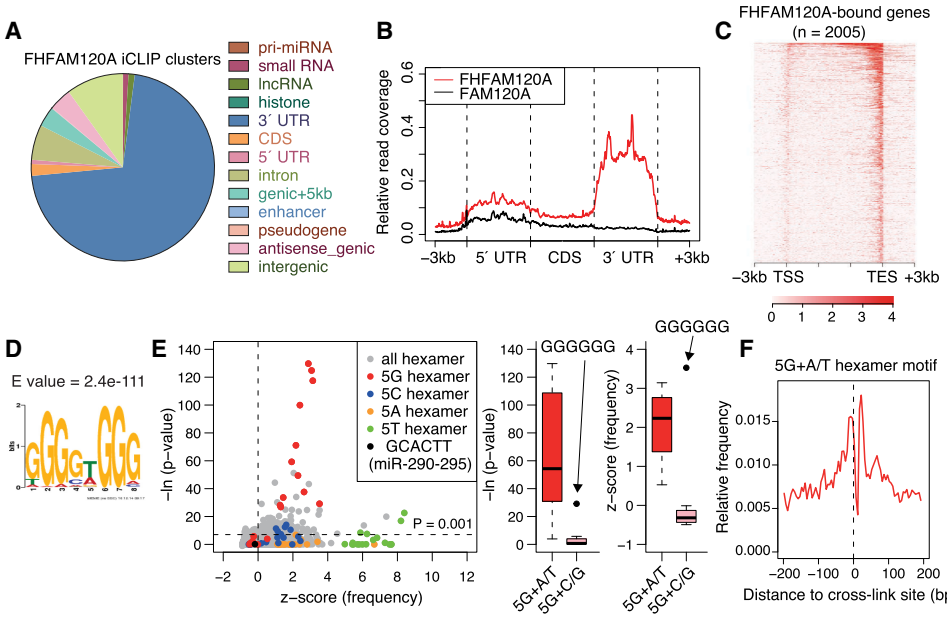

FIGURE 2. iCLIP of FAM120A reveals binding to 3′-UTRs of mRNA and an enrichment of G-rich motifs. (*A*) Breakdown of RNA species bound to FHFAM120A from FHFAM120A iCLIP analysis. (*B*) Localization of FHFAM120A iCLIP clusters within bound mRNAs. A binding profile of untagged FAM120A iCLIP library is shown as a control. (*C*) Heatmap of FHFAM120A iCLIP clusters along mRNA for FHFAM120A-bound genes. (*D*) MEME analysis of the 20 nt sequences flanking the summits of the top 1500 FHFAM120A iCLIP clusters. (*E*) Hexamer enrichment analysis in FAM120A iCLIP clusters. In the *middle* panel, the *x*-axis shows the *z*-scores of hexamer frequency. The *y*-axis shows the negative log *P*-value of statistical significance of the hexamer enrichment *above* background. The *right* panels show a comparison of G-rich hexamers with A/T and C/G. (*F*) Positional enrichment of 5G + A/T motifs around the cross-link sites.

binding, protein localization, nucleotide binding, and regulation of translation (Supplemental Fig. S2C).

Motif analysis of FAM120A-bound RNA sequences using MEME revealed a strong enrichment for poly(G) sequences and weak enrichment of other homopolymeric tracts including poly(C), poly(U), and poly(A) sequences (Fig. 2D; Supplemental Fig. S2D; Bailey et al. 2009). In addition, we analyzed the enrichment of all possible hexamers and found that homopolymeric sequences, especially G-rich motifs, are strongly enriched in FAM120A-bound sequences (Fig. 2E). The G-rich motif also showed cross-link site-centric enrichment (Fig. 2F). This unbiased approach indicates that FAM120A binds to poly(G) sequences in RNAs when assayed on a genome-wide scale.

FAM120A-bound genes are resistant to Ago2-mediated target repression

Next, we investigated the functional relationship between Ago2 and FAM120A. Strikingly, comparison of FAM120A iCLIP and Ago2 iCLIP revealed that greater than one-third of mRNAs bound by Ago2 in mESCs are also bound by FAM120A (Fig. 3A, left; Bosson et al. 2014). However, we observed that only a small fraction of Ago2 iCLIP sites spatially overlaps with FAM120A iCLIP sites (Fig. 3A, right). Consistent with the lack of overlapping binding sites, there was no statistically significant enrichment of 6mer binding sites for highly expressed miRNAs in mESCs in FAM120A iCLIP sites (Fig. 2). This suggested that Ago2 and FAM120A co-bind to many target genes through distinct binding sites, that is, Ago2 through miRNA seed-type binding sites and FAM120A through G-rich motifs, respectively.

As previously reported, TT-FHAgo2 mESCs display Dox-inducible repression of Ago2-bound miRNA target mRNAs (Bosson et al. 2014). By comparing RNA-seq profiles of TT-FHAgo2 mESCs after Dox starvation or treatment with high dose Dox (Bosson et al. 2014), we interrogated the impacts of FAM120A binding on Ago2-mediated target repression. When analyzing either all Ago2-bound miRNA targets or Ago2-bound targets of the highly expressed miR-294, mRNAs bound by both Ago2 and FAM120A showed less target repression relative to mRNAs solely bound by Ago2 (Fig. 3B). This trend was also observed for target genes of the 8 highest expressed miRNAs in mESCs (Fig. 3C), suggesting that avoidance of Ago2-mediated target repression for FAM120A-bound genes is a general phenomenon. In addition, we observed that FAM120A-bound mRNAs are more highly expressed relative to Ago2-bound mRNAs (Supplemental Fig. S3A,B).

FAM120A modulates target genes through G-rich motif

We further analyzed effects of FAM120A binding to 3′-UTRs by utilizing 3′-UTR luciferase reporter assays. To

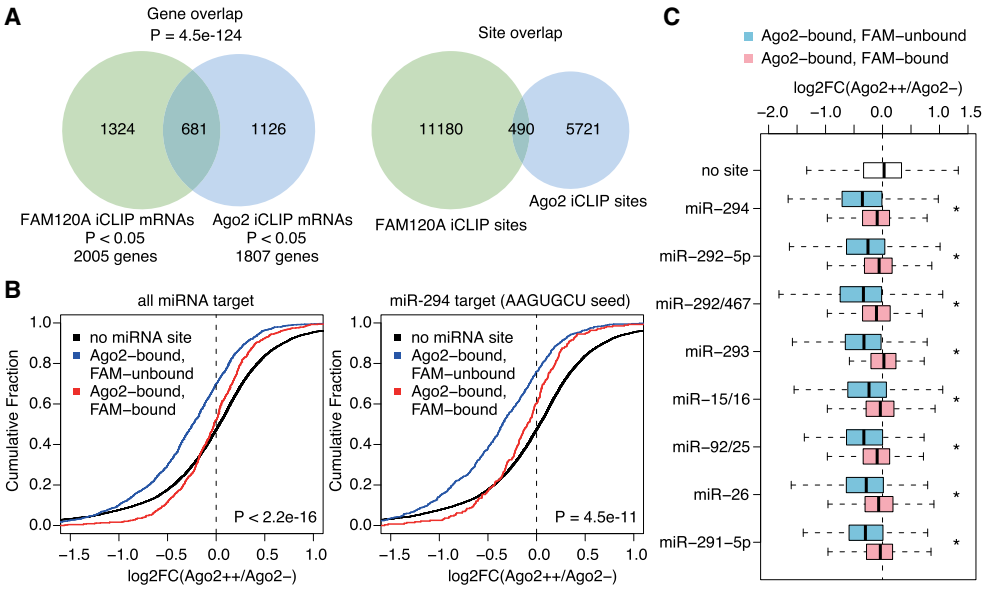

FIGURE 3. FAM120A-bound mRNAs are devoid of Ago2-mediated target repression. (*A*) Venn diagram depicting overlap of FAM120A- and Ago2-bound mRNAs (*left*) and positional overlap of FAM120A and Ago2 iCLIP clusters (*right*). *P*-value is calculated using hypergeometric test. (*B*) Cumulative distributions of fold changes (FC; Ago2 ++ represents 2.5 µg/mL Dox treatment for 48 h, Ago2 – represents Dox starvation for 96 h) of Ago2-bound and FAM120A-bound miRNA target mRNAs and Ago2-bound and FAM120A-unbound miRNA target mRNAs. *Left* and *right* panels show results for all miRNA targets and miR-294 targets, respectively. All of 6mer, 7mer, and 8mer were considered. *P*-values are calculated by two-sided K–S test (Ago2-bound and FAM120A-unbound vs. Ago2-bound and FAM120A-bound). (*C*) Box plot showing fold changes (Ago2 ++ vs. Ago2 –) of Ago2-bound and FAM120A-bound target mRNAs and Ago2-bound and FAM120A-unbound target mRNAs for representative miRNAs highly expressed in mESCs. (*) $P < 0.001$ with two-sided K–S test.

this end, we compared the 3′-UTRs of miR-294 target mRNAs bound by Ago2 but not bound by FAM120A and the 3′-UTRs of miR-294 target mRNAs bound by Ago2 and also containing G-rich motif-positive FAM120A iCLIP sites. In TT-FHAgo2 cells, the former showed potent Dox-dependent repression, while Dox-dependent repression was weaker for the latter (Fig. 4A). On the other hand, in TT-FHFAM120A cells, FAM120A overexpression by Dox treatment did not impact reporters harboring 3′-UTRs that are bound by Ago2 only, but enhanced reporter expression of the reporters harboring 3′-UTRs that are bound by Ago2 and FAM120A, suggesting that FAM120A enhances the expression levels of its bound genes (Fig. 4B). Furthermore, mutagenesis experiments of G-rich motifs bound by FAM120A showed that mutation of G-rich motifs abolishes FAM120A overexpression-mediated reporter expression enhancement (Fig. 4C; Supplemental Fig. S3C). Collectively, these results suggest that FAM120A potentially modulates its target genes through G-rich motifs and FAM120A binding may attenuate Ago2-mediated target repression.

DISCUSSION

The present study identified FAM120A as an Ago2 interacting protein by utilizing mESCs conditionally expressing a single epitope-tagged Ago1 or Ago2 in an all Ago-deficient background (Bosson et al. 2014; Zamudio et al. 2014). In two previously reported Ago2 interactome data sets (Frohn et al. 2012; Schopp et al. 2017), FAM120A has been listed as an Ago2 binding partner, supporting the validity of our findings. However, the functional consequences of FAM120A/Ago interaction have not previously been investigated. Our Ago2 IP mass spectrometry data also included representative Ago2 binding partners such as HSP90 and TNRC6B. Ago proteins interact with a variety of binding partners and appear to exist in multiple protein complexes. A recent conditional proteomics approach using protein fragments complementation and proximity-dependent biotinylation technique (split-BioID) clearly demonstrated that two Ago2 complexes, Ago2–Dicer and Ago2–TNRC6C complexes, are associated with distinct protein partners (Schopp et al. 2017). The former, representative of RLC, is associated with TRBP and HSC70/HSP90, while the latter is associated with other miRISC core components, including TNRC6A, TNRC6B, CNOT4, and other miRISC modulators. In their report, FAM120A is one of Ago2 binding partners, but is not enriched in either Ago2–Dicer complexes or Ago2–TNRC6C complexes (Schopp et al. 2017). In addition, our findings suggest that FAM120A-bound Ago2 target genes are significantly less sensitive to Ago2-mediated target repression. Taken together, Ago2–FAM120A association may represent an additional Ago2 complex, which is not

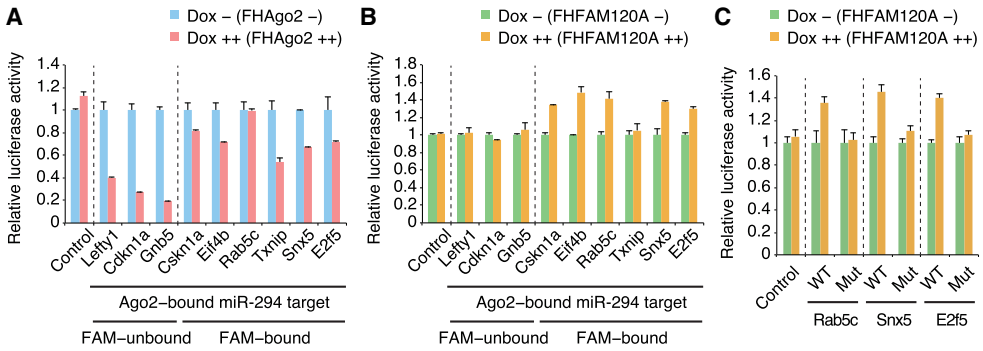

FIGURE 4. FAM120A stabilizes its bound 3′-UTRs through G-rich motifs. (*A*,*B*) 3′ UTR reporter assay of Ago2-bound miR-294 target genes not bound by FHFAM120A or having G-rich motif-positive FHFAM120A iCLIP clusters in TT-FHAgo2 mESCs (*A*) and TT-FHFAM120A mESCs (*B*). mESCs were cultured in the absence (Dox –) or presence (2.5 µg/mL, Dox ++) of Dox for 48 h, transfected with luciferase reporter plasmids, and then subjected to luciferase reporter assays 48 h after transfection. (*C*) Effects of mutation of G-rich motifs on FAM120A-mediated target stabilization in TT-FHFAM120A mESCs. (WT) Wild-type, (Mut) mutant.

functional in miRNA-mediated target repression in the cytoplasm.

FAM120A was initially reported to be a component of Purα-containing mRNP complexes (Kobayashi et al. 2008). Subsequently, it was reported that the carboxyl terminus of FAM120A directly binds to IGF-II mRNA and promotes the extracellular secretion of IGF-II protein (Tanaka et al. 2009). In addition, FAM120A has been reported to be an RNA-binding protein in mESCs (Kwon et al. 2013), but its full cellular RNA-binding properties have not been well characterized. Our iCLIP analysis reveals genome-wide target preferences of FAM120A with striking overlap between Ago2-bound mRNAs and FAM120A-bound mRNAs. G-rich motif enrichment in our FAM120A iCLIP study is also consistent with a previous report showing that FAM120A binds to homopolymeric tracts in vitro (Tanaka et al. 2009).

The functional analysis presented here suggests that FAM120A may attenuate Ago2-mediated target repression through its bound G-rich motifs. While the specific mechanism by which the binding of FAM120A counteracts mRNA degradation is unclear, it is likely independent of binding of the miRNA-Ago2 complex to its targets, as the binding sites of FAM120A and Ago2 do not directly overlap. This suggests that FAM120A may inhibit Ago2-mediated target repression at steps downstream from miRNA binding, for example, by inhibiting recruitment of GW182 proteins or other miRISC partners. This scenario would be consistent with the lack of detectable enrichment of FAM120A in an Ago2–TNRC6C complex (Schopp et al. 2017). Alternatively, it is possible that FAM120A binds to other RBPs, which counteract Ago2-target destabilization. Indeed, using tandem Flag-HA IP mass spec of FHFAM120A in mESCs, we found that FAM120A associates with multiple other RNA-binding proteins, including hnRNP A1, hnRNP A3, hnRNP AB, hnRNP D, IGF2BP1, IGF2BP3, PABPC1, ELAVL1, and YBX1 (data not shown). The association between FAM120A and IGF2BP1 is consistent with a previous report (Tanaka et al. 2009). In HEK293 cells, IGF2BP1 and Ago2 have previously been reported to bind to overlapping mRNA targets, although IGF2BP1-bound transcripts do not show an enrichment in miRNA seed-complementary sites (Landthaler et al. 2008). Given these observations, the association between FAM120A and multiple RNA-binding proteins may serve to counteract Ago2-mediated destabilization of FAM120A-bound target mRNAs.

Ago2–FAM120A association may involve additional roles of Ago2 in the modulation of cancer-related signaling pathways and may be associated with distinct cellular localization relative to Ago2–GW182 complex. Recent reports have shown that Ago2 interacts with various cell signaling pathways and have miRNA-independent functions, especially in cancer biology (Shen et al. 2013; Yang et al. 2014; Shankar et al. 2016). In breast cancer, hypoxia was found to enhance the association between EGFR and Ago2 (Shen et al. 2013). This resulted in EGFR-mediated phosphorylation of Ago2–Y393, which inhibited loading of miRNAs with tumor suppressive properties due to Ago2 structural differences. Furthermore, a direct interaction between KRAS and Ago2 has been recently reported in oncogenic KRAS-driven cancers, as evidenced in multiple lung and pancreatic cancer cell lines (Shankar et al. 2016). This interaction was found to occur on the endoplasmic reticulum and to involve the switch II domain of KRAS and the amino-terminal domain of Ago2. Engagement of KRAS with Ago2 reduced RISC activity and promoted stabilization of oncogenic KRAS. The association between KRAS and Ago2 resulted in enhanced PI3K signaling and promoted cellular transformation (Shankar et al. 2016). Apart from its RNA-binding function, FAM120A has been reported to be a scaffold protein necessary for activation of several intracellular kinases, including Src, FAK, and PI3K, in response to oxidative stress and

IL13 receptor α2 signaling in cancer cells. These interactions are associated with cancer progression (Tanaka et al. 2009; Bartolome et al. 2015). Interestingly, Ago-KRAS association appears to be specific for Ago2 among the four Ago proteins (Shankar et al. 2016), and FAM120A interaction was also specifically observed for Ago2 but not Ago1 in our study. Thus, Ago2–FAM120A interaction may be associated with additional and specific roles of Ago2 in cancer biology.

MATERIALS AND METHODS

Cell culture

TT-FHAgo2 mESCs were maintained as described previously (Zamudio et al. 2014). TT-FHFAM120A mESCs were generated utilizing the pSLIK lentiviral expression system (Shin et al. 2006). Lentivirus was generated in 293T cells by cotransfection with pCMV-dR8.91 packaging and pHDM.G envelope vector. 293T media was collected and filtered through a 0.45 µm syringe and supplemented with 1 mM HEPES pH 7.0. Cells were infected overnight with 4 µg/mL polybrene (Millipore) in a six well dish after centrifugation at room temperature for 1 h at 2000 rpm. Cells were selected with 150 µg/mL hygromycin B in ES cell media to generate stable cells.

Plasmids

3′-UTR reporter vectors were generated by inserting 3′-UTR sequences into the 3′-UTR of the luciferase gene in the psiCHECK-2 dual luciferase reporter vector (Promega) (Suzuki et al. 2015, 2018). Mutations were introduced by a PCR-based approach. Primer sequences are given in Supplemental Table S2.

Argonaute IP

TT-Ago2 (control), TT-FHAgo1, or TT-FHAgo2 cells were induced with Dox (2.5 µg/mL) and fractionated to cytosolic and nuclear fractions. Cytosolic and nuclear fractions were dialyzed in buffer DB (20 mM Tris-Cl pH 8, 10% Glycerol, 100 mM KCl, 5 mM MgCl2, 0.2 mM EDTA) for 6 h with four buffer changes. Dialyzed lysates were centrifuged and Flag IP was carried out overnight with M2 Flag conjugated magnetic beads (Sigma). Immunoprecipitated material was washed and eluted with 3× Flag peptide (Sigma) twice at room temperature. The eluted material was TCA precipitated overnight at 4°C. The precipitate was resuspended in gel loading buffer, separated utilizing 4%–12% SDS-PAGE (Thermo Fisher Scientific), and visualized with Imperial stain (Thermo Fisher Scientific). The gel was separated into eight equal size pieces and submitted to the Biopolymers & Proteomics Core Facility of Robert A. Swanson (1969) Biotechnology Center at the Koch Institute for mass spectrometry.

iCLIP

FHFAM120A iCLIP was carried out after Dox induction (2.5 µg/mL) utilizing tandem Flag and HA IP after UV cross-linking as previously described (Jangi et al. 2014). Data represents the results from one experiment.

Bioinformatics

Analysis of iCLIP libraries was performed as previously described (Bosson et al. 2014). MEME analysis was performed for the 20 nt sequences flanking the summits of the top 1500 iCLIP clusters (Bailey et al. 2009). Hexamer enrichment analysis was performed using the 40 nt sequences flanking the center of iCLIP clusters on both directions, all possible hexamers, and background sequence sets generated by HOMER (v4.10) (Heinz et al. 2010; Grigelioniene et al. 2019). GO analysis was carried out using Database for Annotation, Visualization, and Integrated Discovery (DAVID; https://david.ncifcrf.gov/). Data sets of target genes of all miRNAs were downloaded from the TargetScan database (v7.1; targetscan.org) (Agarwal et al. 2015). We analyzed the data of RNA-seq in TT-FHAgo2 cells with/without Dox treatment (Bosson et al. 2014) using a maximum filter of FPKM > 0.1 or 1. For target gene expression changes, *P*-values were calculated by two-sided Kolmogorov–Smirnov (K–S) test.

Luciferase reporter assay

TT-FHAgo2 or TT-FHFAM120A mESCs were cultured in the absence or presence (2.5 µg/mL) of Dox (Sigma) for 48 h, and then transfected with luciferase reporter plasmids using Lipofectamine 2000 (Thermo Fisher Scientific). Forty-eight hours after transfection, the ratio between firefly and *Renilla* luciferase was determined using Dual-Luciferase Reporter Assay System (Promega).

DATA DEPOSITION

Data generated during this study are available in the Gene Expression Omnibus under accession number GSE128264.

SUPPLEMENTAL MATERIAL

Supplemental material is available for this article.

ACKNOWLEDGMENTS

We are grateful to the members of the Sharp laboratory for discussions and assistance. We thank the Robert A. Swanson (1969) Biotechnology Center at the Koch Institute for Integrative Cancer Research at Massachusetts Institute of Technology for technical support, specifically S. Levine and the staff of the BioMicro Center/KI Genomic Core Facility and R.F. Cook and the staff of the Biopolymers & Proteomics Core Facility. T.J.K. was supported by National Institutes of Health National Research Service Award (NIH NRSA) F32GM101872. H.I.S. was supported by the Uehara Memorial Foundation Research Fellowship and the Osamu Hayaishi Memorial Scholarship for Study Abroad. This work was supported by United States Public Health Service grants R01-GM034277 and R01-CA133404 to P.A.S. from the NIH, and by the Koch Institute Support (core) grant P30-CA14051 from the National Cancer Institute.

Author contributions: T.J.K. and H.I.S. performed the experiments and analyzed the data; J.R.Z. analyzed the data; M.S. performed the experiments; H.I.S. and P.A.S. wrote the paper with contributions from all authors.

Received April 29, 2019; accepted July 1, 2019.

REFERENCES

Agarwal V, Bell GW, Nam JW, Bartel DP. 2015. Predicting effective microRNA target sites in mammalian mRNAs. *Elife* **4:** e05005. doi:10.7554/eLife.05005

Bailey TL, Boden M, Buske FA, Frith M, Grant CE, Clementi L, Ren J, Li WW, Noble WS. 2009. MEME SUITE: tools for motif discovery and searching. *Nucleic Acids Res* **37:** W202–W208. doi:10.1093/nar/gkp335

Bartolome RA, Garcia-Palmero I, Torres S, Lopez-Lucendo M, Balyasnikova IV, Casal JI. 2015. IL13 receptor α2 signaling requires a scaffold protein, FAM120A, to activate the FAK and PI3K pathways in colon cancer metastasis. *Cancer Res* **75:** 2434–2444. doi:10.1158/0008-5472.CAN-14-3650

Bosson AD, Zamudio JR, Sharp PA. 2014. Endogenous miRNA and target concentrations determine susceptibility to potential ceRNA competition. *Mol Cell* **56:** 347–359. doi:10.1016/j.molcel.2014.09.018

Braun JE, Huntzinger E, Fauser M, Izaurralde E. 2011. GW182 proteins directly recruit cytoplasmic deadenylase complexes to miRNA targets. *Mol Cell* **44:** 120–133. doi:10.1016/j.molcel.2011.09.007

Chekulaeva M, Mathys H, Zipprich JT, Attig J, Colic M, Parker R, Filipowicz W. 2011. miRNA repression involves GW182-mediated recruitment of CCR4-NOT through conserved W-containing motifs. *Nat Struct Mol Biol* **18:** 1218–1226. doi:10.1038/nsmb.2166

Fabian MR, Cieplak MK, Frank F, Morita M, Green J, Srikumar T, Nagar B, Yamamoto T, Raught B, Duchaine TF, et al. 2011. miRNA-mediated deadenylation is orchestrated by GW182 through two conserved motifs that interact with CCR4-NOT. *Nat Struct Mol Biol* **18:** 1211–1217. doi:10.1038/nsmb.2149

Frohn A, Eberl HC, Stöhr J, Glasmacher E, Rüdel S, Heissmeyer V, Mann M, Meister G. 2012. Dicer-dependent and -independent Argonaute2 protein interaction networks in mammalian cells. *Mol Cell Proteomics* **11:** 1442–1456. doi:10.1074/mcp.M112.017756

Grigelioniene G, Suzuki HI, Taylan F, Mirzamohammadi F, Borochowitz ZU, Ayturk UM, Tzur S, Horemuzova E, Lindstrand A, Weis MA, et al. 2019. Gain-of-function mutation of microRNA-140 in human skeletal dysplasia. *Nat Med* **25:** 583–590. doi:10.1038/s41591-019-0353-2

Heinz S, Benner C, Spann N, Bertolino E, Lin YC, Laslo P, Cheng JX, Murre C, Singh H, Glass CK. 2010. Simple combinations of lineage-determining transcription factors prime *cis*-regulatory elements required for macrophage and B cell identities. *Mol Cell* **38:** 576–589. doi:10.1016/j.molcel.2010.05.004

Höck J, Weinmann L, Ender C, Rüdel S, Kremmer E, Raabe M, Urlaub H, Meister G. 2007. Proteomic and functional analysis of Argonaute-containing mRNA-protein complexes in human cells. *EMBO Rep* **8:** 1052–1060. doi:10.1038/sj.embor.7401088

Jangi M, Boutz PL, Paul P, Sharp PA. 2014. Rbfox2 controls autoregulation in RNA-binding protein networks. *Genes Dev* **28:** 637–651. doi:10.1101/gad.235770.113

Kobayashi Y, Suzuki K, Kobayashi H, Ohashi S, Koike K, Macchi P, Kiebler M, Anzai K. 2008. C9orf10 protein, a novel protein component of Purα-containing mRNA-protein particles (Purα-mRNPs): characterization of developmental and regional expressions in the mouse brain. *J Histochem Cytochem* **56:** 723–731. doi:10.1369/jhc.2008.950733

Kwon SC, Yi H, Eichelbaum K, Föhr S, Fischer B, You KT, Castello A, Krijgsveld J, Hentze MW, Kim VN. 2013. The RNA-binding protein repertoire of embryonic stem cells. *Nat Struct Mol Biol* **20:** 1122–1130. doi:10.1038/nsmb.2638

Landthaler M, Gaidatzis D, Rothballer A, Chen PY, Soll SJ, Dinic L, Ojo T, Hafner M, Zavolan M, Tuschl T. 2008. Molecular characterization of human Argonaute-containing ribonucleoprotein complexes and their bound target mRNAs. *RNA* **14:** 2580–2596. doi:10.1261/rna.1351608

Li S, Wang L, Fu B, Berman MA, Diallo A, Dorf ME. 2014. TRIM65 regulates microRNA activity by ubiquitination of TNRC6. *Proc Natl Acad Sci* **111:** 6970–6975. doi:10.1073/pnas.1322545111

Schopp IM, Amaya Ramirez CC, Debeljak J, Kreibich E, Skribbe M, Wild K, Béthune J. 2017. Split-BioID a conditional proteomics approach to monitor the composition of spatiotemporally defined protein complexes. *Nat Commun* **8:** 15690. doi:10.1038/ncomms15690

Shankar S, Pitchiaya S, Malik R, Kothari V, Hosono Y, Yocum AK, Gundlapalli H, White Y, Firestone A, Cao X, et al. 2016. KRAS engages AGO2 to enhance cellular transformation. *Cell Rep* **14:** 1448–1461. doi:10.1016/j.celrep.2016.01.034

Shen J, Xia W, Khotskaya YB, Huo L, Nakanishi K, Lim SO, Du Y, Wang Y, Chang WC, Chen CH, et al. 2013. EGFR modulates microRNA maturation in response to hypoxia through phosphorylation of AGO2. *Nature* **497:** 383–387. doi:10.1038/nature12080

Shin KJ, Wall EA, Zavzavadjian JR, Santat LA, Liu J, Hwang JI, Rebres R, Roach T, Seaman W, Simon MI, et al. 2006. A single lentiviral vector platform for microRNA-based conditional RNA interference and coordinated transgene expression. *Proc Natl Acad Sci* **103:** 13759–13764. doi:10.1073/pnas.0606179103

Suzuki HI, Miyazono K. 2011. Emerging complexity of microRNA generation cascades. *J Biochem* **149:** 15–25. doi:10.1093/jb/mvq113

Suzuki HI, Katsura A, Yasuda T, Ueno T, Mano H, Sugimoto K, Miyazono K. 2015. Small-RNA asymmetry is directly driven by mammalian Argonautes. *Nat Struct Mol Biol* **22:** 512–521. doi:10.1038/nsmb.3050

Suzuki HI, Spengler RM, Grigelioniene G, Kobayashi T, Sharp PA. 2018. Deconvolution of seed and RNA-binding protein crosstalk in RNAi-based functional genomics. *Nat Genet* **50:** 657–661. doi:10.1038/s41588-018-0104-1

Tanaka M, Sasaki K, Kamata R, Hoshino Y, Yanagihara K, Sakai R. 2009. A novel RNA-binding protein, Ossa/C9orf10, regulates activity of Src kinases to protect cells from oxidative stress-induced apoptosis. *Mol Cell Biol* **29:** 402–413. doi:10.1128/MCB.01035-08

Treiber T, Treiber N, Meister G. 2019. Regulation of microRNA biogenesis and its crosstalk with other cellular pathways. *Nat Rev Mol Cell Biol* **20:** 5–20. doi:10.1038/s41580-018-0059-1

Yang M, Haase AD, Huang FK, Coulis G, Rivera KD, Dickinson BC, Chang CJ, Pappin DJ, Neubert TA, Hannon GJ, et al. 2014. Dephosphorylation of tyrosine 393 in argonaute 2 by protein tyrosine phosphatase 1B regulates gene silencing in oncogenic RAS-induced senescence. *Mol Cell* **55:** 782–790. doi:10.1016/j.molcel.2014.07.018

Zamudio JR, Kelly TJ, Sharp PA. 2014. Argonaute-bound small RNAs from promoter-proximal RNA polymerase II. *Cell* **156:** 920–934. doi:10.1016/j.cell.2014.01.041